Available online at www.sciencedirect.com
SCIENCE DIRECT®
ELSEVIER
Nuclear Instruments and Methods in Physics Research A 521 (2004) 480–492
NUCLEAR INSTRUMENTS & METHODS IN PHYSICS RESEARCH Section A
www.elsevier.com/locate/nima

Time measurements by means of digital sampling techniques: a study case of 100 ps FWHM time resolution with a 100 MSample/s, 12 bit digitizer

L. Bardelli, G. Poggi*, M. Bini, G. Pasquali, N. Taccetti

INFN and Department of Physics, University of Florence, Via G.Sansone 1, Sesto Fiorentino, 50019 Italy

Received 19 May 2003; received in revised form 13 October 2003; accepted 29 October 2003

Abstract

An application of digital sampling techniques is presented which can simplify experiments involving sub-nanosecond time-mark determinations and energy measurements with nuclear detectors, used for Pulse Shape Analysis and Time of Flight measurements in heavy ion experiments. The basic principles of the method are discussed as well as the main parameters that influence the accuracy of the measurements. The method allows to obtain both time and amplitude information with an electronic chain simply consisting of a charge preamplifier and a fast high resolution ADC (in the present application: 100 MSample/s, 12 bit) coupled to an efficient on-line software. In particular an accurate Time of Flight information can be obtained by mixing a beam related time signal with the output of the preamplifier. Examples of this technique applied to Silicon detectors in heavy-ions experiments involving particle identification via Pulse Shape analysis and Time of Flight measurements are presented. The system is suited for applications to large detector arrays and to different kinds of detectors.

PACS: 29.40.M; 84.30.S; 25.70.Pq; 82.80.R

Keywords: Digital sampling; Time-of-flight measurements; Silicon detectors

1. Introduction

In a recent paper [1] the applicability of digital sampling techniques to particle identification with scintillator detectors has been demonstrated. In the present paper it is shown that the same basic apparatus previously described (a digitizer with 100 MSample/s, 12 bit resolution) makes it possible time-mark determinations with sub-nanosecond resolution. In this way, the sampling method can be applied to Silicon detectors for both particle identification via $\Delta E - E$ and/or Pulse Shape Analysis (PSA) and Time of Flight (ToF) measurements. Extension of the proposed method to coincidence measurements, where accurate synchronization between different detectors is necessary, is also possible.

While the feasibility of high-quality energy measurements, given the 12 bit resolution of the converter, represents a somewhat obvious application

*Corresponding author. Tel.: +39-55-4572249; fax: +39-55-4572121.
E-mail address: poggi@fi.infn.it (G. Poggi).

0168-9002/$ - see front matter © 2003 Elsevier B.V. All rights reserved.
doi:10.1016/j.nima.2003.10.106

of the digitizer, the time-mark determination capability of the device deserves a more detailed illustration because this novel application may constitute a breakthrough for experimental setups involving a large number of detectors, possibly of different types. In fact, the implementation of PSA and sub-nanosecond timing can be obtained merely using a charge preamplifier directly followed by a digitizer, thus greatly simplifying the electronic chain: it is possible to get rid of the slow shaping of the signal and its analog conversion (either peak or charge) and—even more important—the timing electronics, like sub-nanosecond constant fraction and/or leading edge discriminators and TDC conversion. In summary, the technique can be applied to particle identification (charge and mass) with $\Delta E - E$ Silicon—CsI(Tl) telescopes (mainly exploiting the energy resolution performance), to ToF measurements in pulsed beam experiments for mass and energy measurements and to PSA in reverse mounted Silicon detectors. The last two applications mainly rely on both energy and timing performances of the system.

The paper is organized as follows: a simplified overview of the time-mark determination properties of a digital sampling system is presented in the next section, where a definition of the required algorithms is also given. That section also illustrates the modification of the basic algorithms necessary to fully exploit the resolution capability of the system. The expected attainable time resolutions, as estimated by means of detailed simulations, are presented. Section 3 briefly recalls the characteristics of the digitizer used for the time-mark resolution tests. Section 4 shows experimental data presenting the sub-nanosecond timing achieved with the sampling system applied to a Silicon detector for Light Charged Particles (LCP) and Intermediate Mass Fragments (IMF) detection. Sub–nanosecond timing with respect to an external time-reference—like the time mark associated to a pulsed beam—is described in Section 5; results of this approach are shown.

Previous work on extracting time information from digitized sequences, although applied to different experimental situations, can be found in Refs. [2–4].

2. Determination of time marks by means of a sampling system

In order to pin down the main issues involved in the present approach, which consists in extracting one or more time-marks from a digitized signal, we explicitly consider the system that we have also experimentally tested, namely the output of a charge preamplifier connected to a Silicon detector. This approach, while somewhat restricting the generality of the conclusions which can be drawn, permits—on the other side—to realistically consider the noise contribution on the signal (mainly series noise of the input FET).

Given a sequence of digitized samples of a signal (in most cases obtained by a fixed frequency clocked digitizer), the problem of obtaining a time-mark from the signal basically consists of determining the time at which a defined signal amplitude is reached (normally this time does not coincide with any of the sampled points). The time "slicing" provided by the digitizer introduces a natural time scale, which all the time determinations are naturally referred to. Furthermore, since for all practical purposes only time differences are of interest, the best approach to digital time measurements is to deduce all relevant time-differences associated with the signal from the same sequence of digitized samples, which extends sufficiently to cover the whole region containing the needed time marks. In this way the uncertainty associated with the asynchronous sampling of the sequence is removed. This issue will be further addressed in Sections 4 and 5, while in this section the uncertainty of a single time determination attainable with the application of the sampling method is discussed, assuming fixed shape signals and disregarding, for the moment, effects connected to very low-level signals; such effects will be briefly addressed at the end of this section.

In Fig. 1 an idealized output of a charge-preamplifier is shown (thin line; markers indicate the sampling points). Usually, with analog signals, the time mark determination requires an ad hoc Constant Fraction Discriminator module (see for instance Ref. [5]).

In the following we present an algorithm applied to digital samples which permits to define the

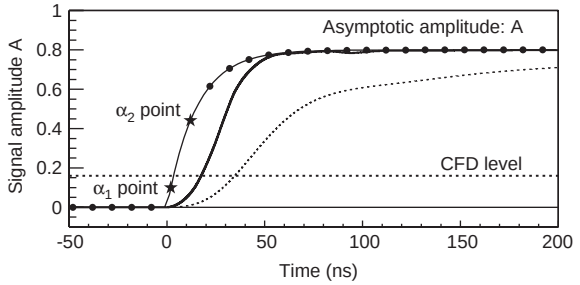

Fig. 1. Solid thin line: schematic representation of the output of a charge preamplifier. Markers: samplings of the signal. Full line: output signal of the used charge preamplifier. Dashed line: preamplifier output distorted by the presence of a long transmission line (see Section 4).

instant of time at which the signal reaches a predetermined fraction f of the full amplitude; we call it digital Constant Fraction Discriminator (dCFD). A simple estimate of the time-mark resolution achievable with that approach is given, mainly to introduce the basic issues associated with digital sampling timing. The estimate will be performed in the basic hypothesis that the time needed for the signal to pass from its zero value to full amplitude (in practice the 10–90% risetime of the signal, briefly *risetime* t_r in the following) contains a few sampling periods τ_{clk}. Moreover, the "first order" assumption of a linear shape of the signal around the chosen threshold region is made (in the following we will extend the results to non-linear behavior). The following notation will be used (see also Fig. 1):

- A asymptotic amplitude of the signal $S(t)$, with $0<A<1$. The value 1 corresponds to the full range of the converter in the chosen configuration.
- τ_{clk} sampling period (in our system $\tau_{clk} = 10$ ns)
- ENOB Effective Number Of Bits of the converter (in our system ENOB = 10.8)[1]
- f dCFD fraction ($0<f<1$)
- t_{dCFD} time at which the amplitude of the signal is fA
- t_r 10–90% risetime of the signal

[1] The Effective Number Of Bits of the converter has been measured and it is in good agreement with the manufacturer's specifications.

A simple way to obtain t_{dCFD} from sampled data is as follows:

(1) Determine the asymptotic amplitude A of the signal, for example with a simple average of the samples at time $T \gg t_r$, after having subtracted the baseline determined from the sample points preceding the signal.
(2) Find the two consecutive samples with amplitudes α_1 and α_2 such that $\alpha_1 < fA < \alpha_2$ (see Fig. 1).
(3) Obtain t_{dCFD} with a linear interpolation between (t_1, α_1) and (t_2, α_2) (note: $t_2 - t_1 = \tau_{clk}$).

Following this procedure, the contribution to the time resolution due to this approach (i.e. the error σ_{dCFD} on t_{dCFD}) can be estimated as:

$$\sigma_{dCFD} \leqslant \sigma_{e+q} \left[\left| \frac{dS}{dt} \right|_{t_{dCFD}} \right]^{-1}$$

$$\sigma_{e+q}^2 = \sigma_e^2 + \frac{1}{12 \times 4^{ENOB}} \quad (1)$$

where σ_e^2 is the variance associated with the electronic noise of the preamplifier (assuming white noise for the sake of simplicity). The quantization error has been considered using the ADC number ENOB of *effective* bits, according with its definition. The error on A has been neglected, because it can be sufficiently reduced by using a proper algorithm (for example averaging over a large number of samples), as well as the error on τ_{clk} (this error amounts to less then few ps with a proper electronic design).

The equality sign in Eq. (1) holds in the limiting case of a value fA coinciding with one of the two samples or when the two amplitude determinations α_1 and α_2 are fully correlated; in the opposite case of total independence of errors, the minimum value of the left member is obtained when $fA = (\alpha_1 + \alpha_2)/2$.

The nominal resolution attainable with an analog CFD treatment of the signal (assuming the same noise bandwidth) is given by an expression identical to Eq. (1), except for an equal sign, for the absence of the quantization error and for an additional factor $\sqrt{1+f^2}$ coming from the

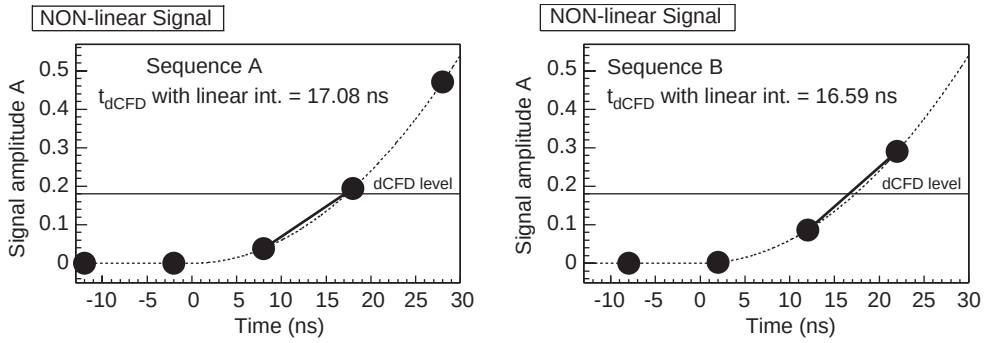

Fig. 2. Two different ideal (noiseless) samplings of the *same* signal with a *non-linear* time dependence. Sequences A and B have a different phase with respect to the signal. The linear interpolation procedure for determining t_{dCFD} produces significantly different values for the two cases. The example refers to a 100 MSample/s digitizer.

signal treatment performed in the CFD electronic module.

It is worth stressing that, if the quantization error is significantly lower that the electronic noise, i.e. if the number of effective bits is sufficiently high to keep the electronic noise of the signal as the dominant effect in the amplitude determination, signals *evolving linearly as a function of time* show a dCFD time resolution better or equal to that attainable with analog CFD module. This result actually means that the key issue for dCFD resolution is the number of effective bits necessary to confine the quantization error below the electronic noise of the signal, while the sampling period τ_{clk} must be sufficiently short to allow for the presence of some samples during the risetime of the signal. As it will be quantitatively shown in the following, the FWHM resolution can be as low as $\sim$100 ps for a proper choice of the used converter.

In the previous discussion the time mark resolution of a digital sampling system has been estimated, assuming a linear shape of the signal near t_{dCFD}. However, the non-linear shape of the signal and the use of an asynchronous (with respect to the signal) clock of period τ_{clk} produces a random error in the interpolating procedure, which translates in a degradation of the overall time-resolution. In fact, while for a signal having a *linear* time dependence around the threshold the linear interpolation procedure is free of systematic errors related to the phase of the sampling, this feature is lost once the signal has a *non-linear* time dependence. Fig. 2 shows the different t_{dCFD} values which are observed for a signal with a *non-linear* time-dependence near t_{dCFD}, once two sampling sequences are considered, differing for a time shift. The linearly interpolated t_{dCFD} differs by about 500 ps between the two cases. Due to the random distribution of the sampling phase with respect to the signal, this effect significantly deteriorates the overall time resolution. Although much smaller than the sampling period τ_{clk}, this error can easily overcome the limiting resolution of the sampling system calculated before. Moreover, it depends strongly on the shape of the signal in the proximity of t_{dCFD} and in general does not cancel out when the difference between two distant points of the same signal is performed (e.g. two digital constant fraction timings with different f values).

In order to quantitatively show the worsening of the resolution associated with this effect a simulation has been implemented. The results of the simulation are presented as a function of the risetime of the preamplifier; while in the PSA application presented in the following a few fraction values have been used to estimate the risetime of the signal, the simulations have been run with a representative value $f = 0.2$. A true preamplifier output has been considered and its shape is reported as a full solid line in Fig. 1: it mainly differs from the idealized curve by the non-linear onset of the signal. The reported behavior

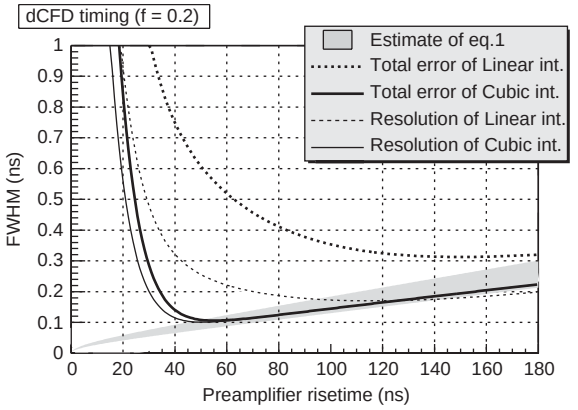

Fig. 3. Total error on digital Constant Fraction timing ($f = 0.2$) as a function of the preamplifier risetime, obtained with a 12 bit resolution, 100 MSample/s digitizer, using linear interpolation (thick dashed line) and cubic interpolation (thick full line). The thin dashed and full lines report, for linear and cubic interpolations respectively, the only time resolution (fluctuations with respect to the average value, for each value of preamplifier risetime). The shaded area represents the range for the resolution expected on the basis of Eq. (1). The simulation has been performed using realistic signals of amplitude equal to half of the range of the converter.

represents the δ-response of the preamplifier output ($t_r \approx 30$ ns) used in the experimental tests presented in the next sections.[2] The electronic noise at the preamplifier output was assumed to have the same amplitude and spectral density that we measured in our experimental set-up. The different risetimes t_r are obtained by a simple scaling on the horizontal axis, keeping the overall shape; the electronic noise has been correspondingly changed, namely the associated full variance increases with the transmitted bandwidth as $\sigma_e^2 \propto 1/t_r$. The digitizer was assumed to have 12 bit resolution and sampling rate of 100 MSample/s, with a sharp antialiasing filter cutting at the Nyquist frequency of 50 MHz.

The shaded region in Fig. 3 represents the limits determined by Eq. (1) for $f = 0.2$ and a signal amplitude of half range ($A = 0.5$). The thick dashed line represents the absolute error (systematic and statistical) with respect to the true value once t_{dCFD} is determined with a linear interpolation. Apart from the expected rapid increase of the error at shorter risetimes, due to the insufficient number of interpolating points, a significant increase of the error with respect to the estimate of Eq. (1) is apparent, even in regions where lacking of interpolating samples can be excluded.

A solution to the problem can be found by using either a fit or a higher order interpolation. The interpolation procedure is preferred over the fitting because it does not rely on any assumption on the shape of the signal and it can usually be computationally faster.

We have successfully tested a cubic polynomial interpolation based on the Lagrange formula. Parabolic interpolation has also been tested, with poorer results with respect to the cubic one. The main reason is that in most cases, especially for fast evolving signals, they present a flex over the few examined samples, which cannot be reproduced by a second order polynomial. The method extends the previously discussed results and proceeds as follows (using the adimensional time variable $x = \text{time}/\tau_{clk}$):

- A time mark $x_{dCFD,linear}$ is obtained with the procedure previously outlined.
- Four adjacent samples x_1, x_2, x_3 and x_4 are chosen, with $x_2 < x_{dCFD,linear} < x_3$ and the unique third-order polynomial $y(x - x_2)$ through them is computed.
- The time x_{dCFD} can be obtained solving the equation $y(x - x_2) = fA$. Numerically this can be done using a successive approximation method (for example the Newton's one) with $x_{dCFD,linear}$ as initial guess. It was verified that, with realistic signals, the iterative solution of this equation converges very fast and thus in many cases the iterative loop can be replaced with a single correction, thus coinciding with a first-order approximation of $y(x - x_2)$ around the point $x_{dCFD,linear}$ (the next approximation step typically introduces a correction smaller than 10–20 ps).

The presented method is well suited for on-line processing of data with DSP, because the

[2] The effect of a long transmission line that during the experimental tests we were forced to insert between the preamplifier output and the input of the digitizer will be addressed in the following sections.

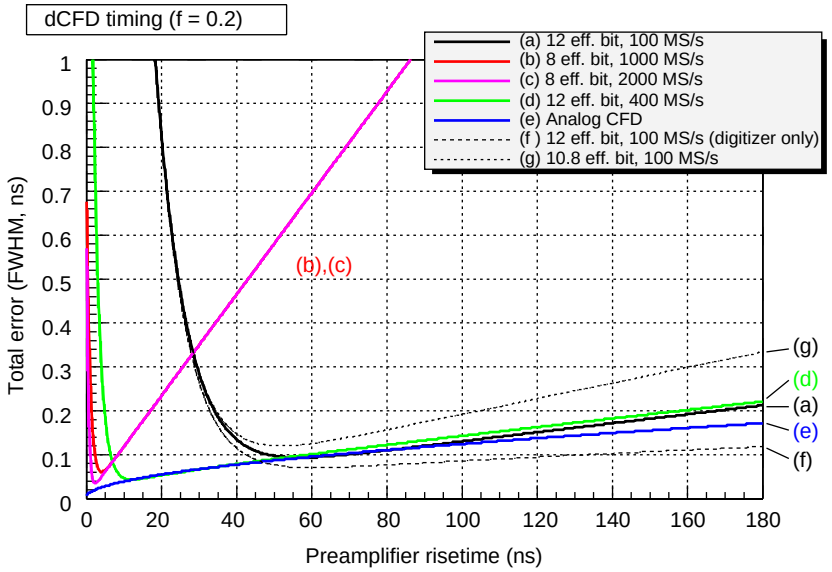

Fig. 4. Total error on digital Constant Fraction timing ($f = 0.2$) performed by various digital sampling systems (continuous lines labeled from *a* through *d*). Data corresponding to a standard analog CFD signal treatment are also shown (continuous line *e*). For one of the digitizers (100 MSample/s-12 bit) the contribution due to digitization only is separately presented (dashed line *f*). The dotted curve *g* refers to the digitizer used in our tests. The simulation has been performed using realistic signals of half full range amplitude ($A = 0.5$).

computation of the correction involves about 15 multiply accumulate (MAC) operations to obtain the coefficients of the polynomial, and 10–20 additional operations to obtain the desired correction.

The thick full line in Fig. 3 represents the results obtained by performing the described cubic interpolation The improvement with respect to the first-order linear interpolation is apparent and the data fall in the shaded region, as expected. The three quantities reported in Fig. 3 and discussed since now refer to the total absolute error with respect to the true value. When the timing information is used for discrimination purposes (like for PSA, see Section 4) only the fluctuations with respect to the mean observed value are of interest. The thin full and dashed curves in Fig. 3 represent indeed these resolutions (for $f = 0.2$) for cubic and linear interpolations, respectively. We have verified that, while the details of the basic signal shape may influence the behavior of the curves in the region of the steep increase of the total absolute error towards short risetimes, the conclusions which can be drawn from Fig. 3 about the quality of dCFD timing with a 100 MSample/s-12 bit digitizer are quite general.

To better pin down the digitizer characteristics which indeed determine the timing quality attainable with digital Constant Fraction Discrimination, further simulations similar to those presented in Fig. 3 have been run for digitizers with different characteristics. The total absolute time mark errors are shown in Fig. 4, together with the results simulated for an ideal analog CFD timing. The considered digitizers, apart from the one that we have developed (100 MSample/s-10.8 effective bit), are a 100 MSample/s-12 eff. bit, 1 GSample/s-8 eff. bit, 2 GSample/s-8 eff. bit and a 400 MSample/s-12 eff. bit. In the simulation the signals are processed by the digitizers, each having an antialiasing filter cutting at the corresponding Nyquist frequency. The risetime of the preamplifier, as well as the corresponding noise, have been varied as already discussed. Fig. 4 confirms that, apart from the very fast risetime region, the key feature for determining the timing quality is the digitizer bit resolution. It is worth noting that both the 12 bit digitizers give timing performances

equivalent to the standard analog CFD timing, while for the faster ADCs the increased sampling rate cannot compensate for the poorer bit resolution. Finally, for the 100 MSample/s-12 bit digitizer the dotted line reports the contribution to the absolute error due to the quantization effects (including effective bits) and actually this represents the ultimate resolution attainable with this converter in the non-realistic hypothesis of a noiseless preamplifier output.

In the special case of very fast AD converters the standard oversampling technique [6] may be applied to increase the overall bit resolution: the signal is sampled by the ADC at a much higher rate f_s than the required Nyquist frequency f_{Ny}. Averaging over the collected data allows for an increase of the resolution of the system by a factor $\sqrt{f_s/(2f_{Ny})}$. For example, the oversampling of a signal with an 8 effective bit, 2000 MSample/s digitizer down to 100 MSample/s gives an improvement by a factor ~ 4.5, i.e. of about 2 bits: the final effective resolution of about 10 bits is still worse than a "true" 100 MSample/s, 12 (and also 10.8) effective bit converter. Moreover it has also to be noted that oversampling requires a *white* input noise for proper effective operation.

The presented simulated results of the dCFD algorithm has been limited to a fixed value of signal amplitude $A = 0.5$. While the time resolution obviously scales as $\sigma_{dCFD} \propto 1/A$ (see Eq. (1)), the behaviour of the centroid of the estimated time distribution as a function of A, i.e. the *time walk*, has been studied by means of the same simulations previously discussed. For the case of our converter (100 MSample/s, 10.8 eff. bits) the results are reported in Fig. 5. The total time walk of the system comes out to be less than 120 ps for a dynamic range of 250: this value compares well with the performances of standard analog CFD systems. Very similar results have been obtained using linear interpolation.

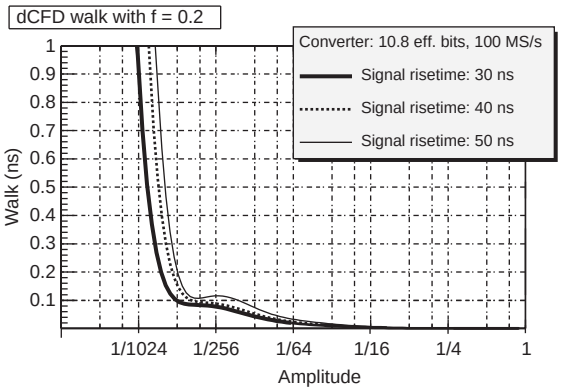

Fig. 5. dCFD walk for a 100 MSample/s, 10.8 eff. bits converter and fraction $f = 0.2$ as a function of signal amplitude A. Note the logarithmic horizontal axis. The three curves correspond to different risetimes (10–90%) of the input signal. For this converter the signal risetime value $t_r = 50$ ns corresponds roughly to the minimum of curve g in Fig. 3.

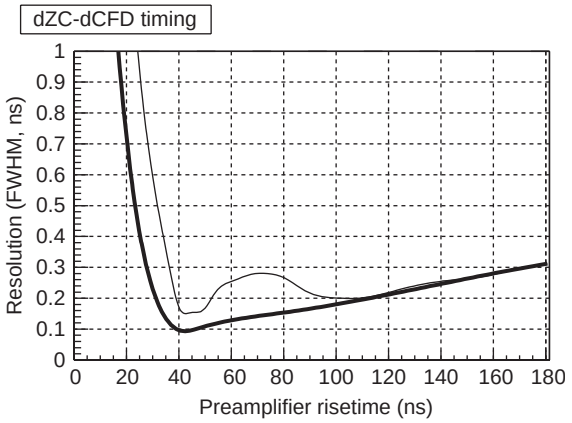

Fig. 6. Resolution (fluctuation with respect to average value) obtained for a Pulse Shape related timing (dZC-dCFD time, see text) from the simulation for linear (thin line) and cubic interpolation (thick line).

The overall time resolution of a single dCFD, as determined by simulations, cannot be easily tested experimentally and the difference of two time determinations is rather needed: as a matter of fact, in Section 4 the Pulse Shape capability of the system is checked by studying the difference between two time marks—the dCFD with $f = 0.2$ fraction and the Zero Cross of the digitally differentiated (delay-line–like) signal, indicated henceforth with "dZC-dCFD". In order to realistically compare simulations with data, Fig. 6 presents the simulated FWHM for the dZC-dCFD time information (for the experimental data see Fig. 8), as a function of preamplifier risetime. The thick line represents the fluctuation with respect to average value, obtained with cubic interpolation, whereas the thin one refers to linear interpolation.

As compared with the behavior of the thin dashed line of Fig. 3 which represents the resolution of a single time determination, the FWHM of the dZC-dCFD difference obtained with linear interpolation presents some compensation effects for short risetimes: in these cases the two time determinations, being based on almost the same samples, are strongly correlated in a way dependent on signal details. Anyway, the resolution for linear interpolation is always worse than the one corresponding to cubic interpolation which, on the contrary, is almost free of any odd behavior because of the better reproduction of the signal shape. Besides, when comparing the performances with experimental data, it will be shown that the resolution worsening due to the linear interpolation procedure also corresponds to a non-Gaussian shape of the timing peak.

According to the results presented in this section, the timing information from our experimental data shown in the next sections has been always extracted by means of the cubic interpolation procedure.

3. The digitizer

In this work the digitizer already described in Ref. [1] has been used: the system is provided with four independent input channels, each sampled by a fast Analog to Digital Converter (ADC, AD9432 from Analog Devices) with a resolution of 12 bit and 100 MSample/s. Specific measurements have determined the effective number of bits as ENOB = 10.8. The analog input stage of each channel is a 3-poles active Bessel filter, that operates as antialiasing filter while minimizing signal distortion. The sampled data is stored on a temporary memory (FIFO) and the full sample is then transferred to the acquisition system through the VME bus: an analysis of the acquired waveform can then be performed off-line. As discussed in Ref. [1] and in the following, all the proposed algorithms are simple and fast enough to be used for on-line analysis with Digital Signal Processors (DSPs). Tests performed with a calibrated pulse injected into a Silicon detector preamplifier have shown that the digitizer does not introduce any deterioration of the energy resolution with respect to the value obtained with standard (spectroscopy grade) analog electronic chain, once the proper algorithms are applied, like semigaussian digital filters.

4. Timing tests with a digital system

In order to verify the timing resolution of the digital sampling system, a test has been performed at the Laboratori Nazionali di Legnaro of INFN (Padova, ITALY) using the $^{16}O + ^{116}Sn$ reaction at a beam energy of 250 MeV. A 300 μm Neutron Transmutation Doped (NTD) Silicon detector has been placed inside a scattering chamber (about 1 m from target, $\theta \simeq 11^\circ$) in the reverse field configuration. The total active area is $\approx 700\ mm^2$; the presented results were obtained with a centered circular collimator, which reduced the exposed area down to $\approx 500\ mm^2$. The detector (nominal depletion voltage of 120 V) has been operated at 140 V. The preamplifier used in all the reported measurements was the one described in Ref. [7], but for an input FET follower stage. The preamplifier, due to its low power consumption, operates in vacuum. The risetime of the preamplifier output for a δ-like excitation is ≈ 30 ns. A 50 m long cable (RG58) connecting the output of the detector preamplifier to the digitizer deteriorates the intrinsic risetime. The resulting shape of the signal at the input of the digitizer is shown in Fig. 1 as a dashed line. The very slow component appearing in the second part of the signal ($t \gtrsim 80$ ns), associated to the response function of the cable, very marginally influences the time information for fractions of the signal smaller than about 0.5 as those which are involved in the present tests (see the following). Practically that means that the effective (with reference to the discussed results) risetime of the preamplifier is about 60 ns, i.e. twice the 10–50% time. Anyway, the final implementation will be provided with shorter cable connections to better exploit the preamplifier characteristics, mounting the digitizers next to the scattering chamber.

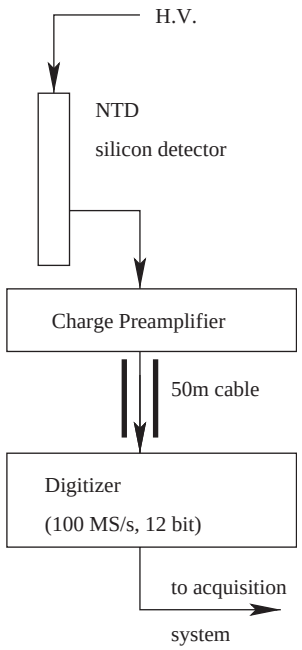

Fig. 7. Electronic chain used for the timing test with pulse-shape analysis. The Silicon detector is mounted in the reverse field configuration. The electronics needed to trigger the acquisition has not been shown.

It is well known (see for instance Ref. [8]) that the shape of the signal from a Silicon detector contains information about the type of the detected particle; moreover the rear side injection technique [9,10] increases the dependence of the shape of the signal on the charge (and even the mass) of the impinging particle, because the effects on the pulse shape due to the high ionization density are enhanced in the lower field regions probed by stopped particles. Therefore, the use of PSA techniques in the ΔE detector of a standard $\Delta E - E$ Silicon telescope permits the identification of particles that are fully stopped in the ΔE detector, thus considerably lowering the thresholds of the system. Good resolution in both energy and time is required for this kind of application, as well as a good doping uniformity of the chosen detector [11].

To perform the test, the simple electronic chain shown in Fig. 7 has been employed: for each event the signal from the detector has been sampled (total sampling time: 10 μs) and transferred to the acquisition system.

The offline analysis performed on the collected waveforms will be discussed in detail in a future paper [12]. Briefly, for each event:

- The asymptotic amplitude A (see Section 2) of the signal has been determined using a moving average filter [13].
- A digital constant fraction (dCFD, with $f = 0.2$ and cubic interpolation) time mark has been obtained.
- A digital zero crossing (dZC) time mark has been obtained applying a digital Delay-Line-like shaping ($t_{DDL} = 100$ ns) to the signal, and computing the zero-crossing time with a simple generalization of the dCFD algorithm.
- A quantity proportional to the energy released in the detector has been computed using a digital shaping of the signal (semigaussian $CR-(RC)^4$ digital filter [13,14] with $\tau = 2$ μs).

All the proposed algorithms are well suited for fast on-line processing of data. Given the used time constants for amplitude and time mark determinations and the intensity of particles impinging on our detector during test runs (about 10^4/s), no optimization of the algorithms has been done with respect to counting rate effects. The use of the zero-crossing algorithm to obtain the second time mark for the PSA is just one possible choice and it

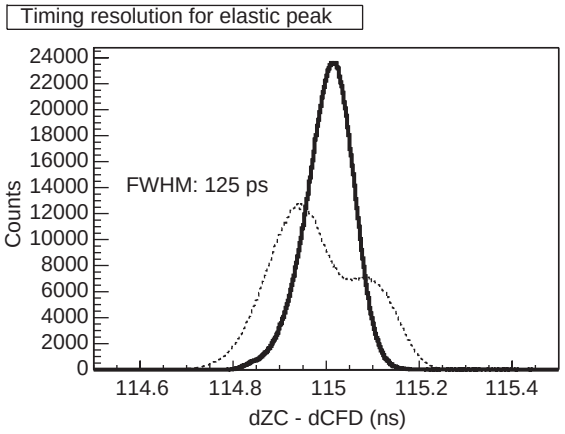

Fig. 8. Full line: dZC-dCFD time spectrum (see text) for the elastic peak as obtained with the digital sampling system as in Fig. 7 and cubic interpolation. Dashed line: the same quantity obtained using linear interpolation: note the strongly non-Gaussian shape of the peak and the worse resolution.

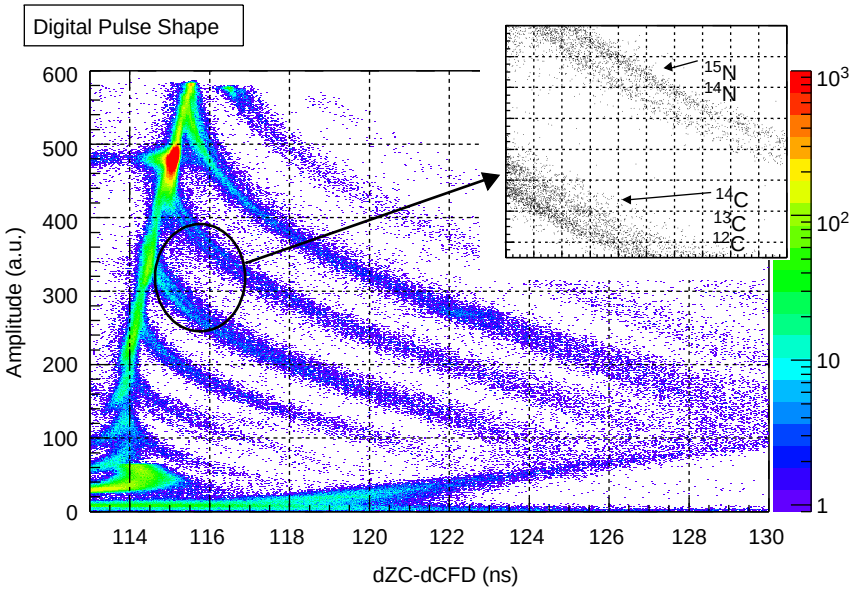

Fig. 9. Digitally determined Amplitude vs. dZC-dCFD time correlation: charge identification is apparent. In the inset: detail of the isotope separation of carbon and nitrogen. Data have been obtained with the electronic chain of Fig. 7.

can be easily replaced by the determination of the time associated to another dCFD having a larger fraction (typically 0.5–0.6). This point will be discussed in Ref. [12].

The obtained results are shown in Fig. 8: the difference dZC-dCFD ($f = 0.2$) for elastic events is shown. At the used bombarding energy of 250 MeV the elastically scattered ^{16}O particles are not stopped in the Silicon detector. The FWHM of the elastic peak is 125 ps. In Fig. 8 the timing spectrum obtained for the same events with a linear interpolation is also shown: as anticipated in Section 2 this low-order interpolation not only affects the overall timing resolution, but produces a strongly non-Gaussian shape. These data are in agreement with the results of the realistic simulation presented in Fig. 6, for $t_r \approx 60$ ns.

In Fig. 9 the overall pulse-shape correlation is shown: the amplitude of the digitally shaped signal is reported against the difference between the digital zero crossing time dZC and the digital constant fraction (dCFD) time mark. One clearly sees that the system is able to discriminate between different particles with full charge resolution. The expanded view makes it possible to also appreciate the existence of a somewhat marginal mass resolution. The energy resolution (electronic contribution plus counting rate effects) on the vertical axis was measured to be about 100 keV, estimated by means of a calibrated charge injected into the preamplifier during the measurements. The counting rate was about 10 kHz. Independent tests performed on the same detector with low energy α particles and proton bursts [7] have shown that the discrimination obtained, mainly for short range highly ionizing particles as those in the right side of the figure which explore only low electric field regions, is limited by the non-homogeneities of the silicon doping [12].

5. A novel approach to Time of Flight measurements

The previous discussion on the timing performances of the digitizer suggests the possibility for such a system to be used for Time of Flight measurements in those cases where a timing resolution of $\sim$100 ps FWHM can be tolerated (i.e. a major part of heavy ions and nuclear physics experiments). As a matter of fact, we have devised a new approach to ToF measurements, based on

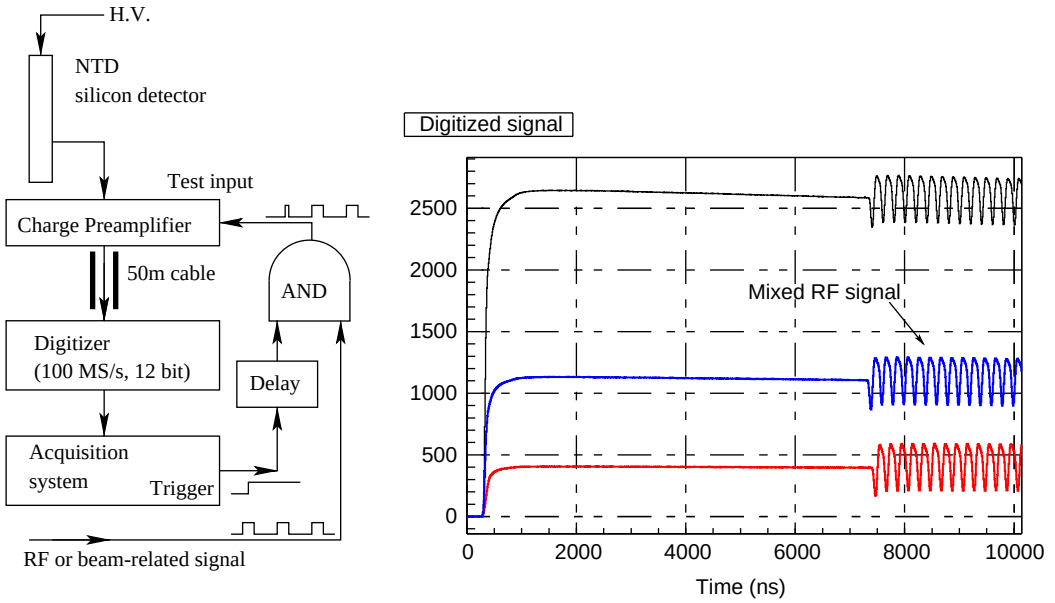

Fig. 10. Left panel: electronic chain employed for mixing a beam related signal with the signal coming from the detector. Right panel: some signals collected using this electronic chain. The system performs energy, pulse-shape and ToF measurements at the same time.

the mixing of a beam related time signal with the to-be-sampled preamplifier output.[3] On the left side of Fig. 10 the electronic chain used in our tests is shown. It could be easily implemented without introducing any change neither in the preamplifier nor in the digitizer: a beam related time signal (for example the Radio Frequency RF signal for pulsed beams) is gated with a delayed ($\sim$7 μs) copy of the general trigger of the experiment and injected in the test input of the preamplifier. On the right side of Fig. 10 some examples of signals acquired with this electronic chain are shown: the mixed RF signal (5 MHz) appears on the tail of the signals coming from the preamplifier. To get digitized sequences like the ones shown in the right side of Fig. 10, an alternative and more versatile solution exists, consisting in the addition of a summing node at the digitizer input for merging together the untouched preamplifier output and the gated time reference signal. Anyway, regardless to the solution adopted for the mixing, the RF time reference does not affect the first part of the signal: the analysis of the preamplifier output can still be performed, as long as the whole interesting physical information (signal amplitude, rise time, shape details) is confined in the first few microseconds. Moreover the ToF of the detected particle can be obtained, apart from an overall offset as usual, as the difference between the mixed RF signal time and the starting time of the preamplifier output (e.g. obtained with a digital Constant Fraction algorithm, as already described). Because of the use of a simple AND gate, the first pulse of the mixed RF signal must be discarded: both its starting time and width depend on the relative overlap between the trigger pulse and the RF signal. Any of the following RF periods can be used for the determination of a beam related time mark: a better time determination is obtained by using an average over all periods (taking into account the associated time-shifts corresponding to integer multiples of the RF period).

Measurements have been performed to test the feasibility of this technique, using the electronic chain of Fig. 10.

Unfortunately the intrinsic time resolution of the ^{16}O beam as measured with a small fast plastic

[3] This application has been briefly described in Ref. [15].

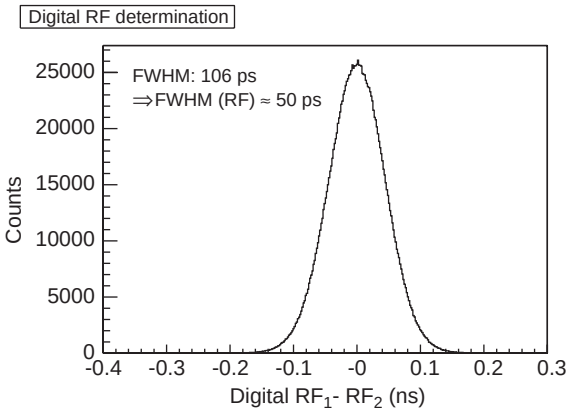

Fig. 11. Distribution of the difference between the two digital RF time mark determinations RF_1 and RF_2 (a common offset has been subtracted). Using the full RF train a resolution of 50 ps FWHM is deduced (see text).

detector and standard fast electronics was about $\sim$1.3 ns FWHM. The same resolution value is obtained with our technique; however, this value is much larger than the expected contribution arising from the digital timing technique, thus preventing a direct comparison with the estimate of Section 2. To perform this comparison the time mark related to the RF signal has been extracted in two independent ways for each event, using two different sets of oscillations: with reference to Fig. 10 (right panel), the first five periods (the last 5) of the RF train have been used to evaluate the time mark RF_1 (RF_2). The distribution of the difference between these two determinations is shown in Fig. 11. The FWHM of the difference is 106 ps. Under the realistic assumption that the fluctuations of the 10 considered determinations are independent, the difference between RF_1 and RF_2 has a standard deviation differing by a factor $\sqrt{2/5}$ from that of a single determination and two times larger than the one obtained from the total average over 10 values. Therefore one extrapolates a FWHM(RF) of the total average of $\approx$50 ps. Of course this figure can be further reduced by increasing the number of oscillations contained in the mixed RF train. In practice this means that, besides the resolution of the pulsed beam, the limiting value to the ToF resolution is of the order of 100 ps, given by the time mark extracted from the detector signal, namely the one associated with the dCFD.

The poor time quality of the beam pulse did not permit to check other important features connected with the determination of the time-mark of the signal, too. In fact, the residual dependence of the obtained time-mark on the signal shape is not only expected to be present, but also enhanced by the rear-side injection of the particles requested by PSA. Such effects—common to any signal time-analysis, analog or digital—would hinder a proper determination of the ion velocity. To that purpose a Silicon Detector mounted with the high field side faced to the impinging particles would be definitely preferable and would guarantee a better shape independence. All these items, together with the optimization of the time resolution of dCFD as a function of the fraction f, are beyond the scope of the present paper and will be deferred to the next planned step of studying the dCFD timing performances in coincidence and lifetime measurements with independent detectors [12].

With reference to that application, it is worth stressing that the presented solution involving RF mixing in the digitized samples, implemented to introduce an external time-reference mark for ToF applications, can be easily extended to permit coincidence measurements between different detectors: in fact, once in all digitized sequences associated to various detectors a common time reference mark is introduced at the analog level (either in the preamplifier input through capacitive injection or at the ADC input by means of a summing node) the time difference of all signals with respect to this common reference is obtained, at the expenses of a small deterioration of the time resolution—see discussion before. From that it immediately follows that also the time differences amongst all fired detectors are available and multiple coincidence measurements can be performed. Systematic effects on timing, like *walk* and counting rate sensitivity, common to all standard coincidence measurements, deserve—as anticipated—a careful and quantitative study.

6. Conclusions

In this paper the use of fast digital sampling techniques for nuclear physics timing measure-

ments has been discussed. Some simple calculations and realistic simulations described in Section 2 show that a sampling system, if provided with an adequate bit resolution and proper interpolating software (cubic dCFD), is able to reach a timing resolution much smaller (about two orders of magnitude) than the sampling period. Specifically, as long as the signal develops on a time interval longer than the sampling period, the sampling period itself plays a minor role in the overall digital time resolution, which—at the contrary—is mainly determined by the number of effective bits of the converter. The results obtained using a 100 MSample/s, 12 bit converter have been presented: the performed tests (using a 300 μm Silicon detector with a $^{16}O + ^{116}Sn$ reaction at a beam energy of 250 MeV) have shown that the timing resolution of this digital sampling system can be as low as ~ 100 ps FWHM, for both pulse-shape and Time of Flight applications. This sampling system is well suited for application to a large number of detectors: the used ADC chip provides relatively low cost, low power and higher resolution characteristics, as compared, for example, with high sample rate commercial systems (as digital oscilloscopes).

In our laboratory the prototype a new modular digital sampling system is under test. It consists of a single unit VME module, provided with eight 125 MSample/s, 12 bit sampling channels: each channel is self-triggerable (using a programmable leading-edge discriminator) and it is provided with a fixed-point DSP processor (ADSP2189N) for on-line treatment of data. The system will also be provided with the possibility of mixing in all digitizers a common external time reference signal (e.g. a train of pulses), aimed at synchronizing all the sampled sequences on the same event to perform sub-nanosecond timing between all detectors fired in an event. This avoids the somewhat cumbersome mixing at the test input of the preamplifiers. The mixing of preamplifier output and time reference signals at the ADC input will be provided with a linear gate option meant to exclude the preamplifier output before introducing the common time reference to all digitizers. This feature guarantees a stable level to the reference signal, regardless of the detectors' counting rate. The synchronization can be also obtained by driving all the ADCs with a unique sampling clock, although this implementation can be technically more complicated.

More tests are actually under way with different detectors, as the Single Chip Telescope [16], with encouraging results: these new data will be reported in a future work [12].

Acknowledgements

Thanks are due to the GARFIELD collaboration for the assistance provided during data taking. Helpful discussions with A. Olmi are kindly acknowledged.

References

[1] L. Bardelli, et al., Nucl. Instr. and Meth. A 491 (2002) 244.
[2] D.G. Cussans, H.F. Health, Nucl. Instr. and Meth. A 362 (1995) 277.
[3] A. Geraci, G. Ripamonti, Nucl. Instr. and Meth. A 422 (1999) 337.
[4] M.A. Nelson, et al., Nucl. Instr. and Meth. A 505 (2003) 324.
[5] G.F. Knoll, Radiation Detection and Measurement, 3rd Edition, Wiley, New York, 1999.
[6] Improving ADC Resolution By Oversampling and Averaging, CYGNAL Application note AN018, available on www.cygnal.com.
[7] N. Taccetti, et al., Nucl. Instr. and Meth. A 496 (2003) 481.
[8] C.A. Ammerlaan, et al., Nucl. Instr. and Meth. 22 (1963) 189.
[9] G. Pausch, et al., Nucl. Instr. and Meth. A 365 (1995) 176.
[10] M. Mutterer, et al., IEEE Trans. Nucl. Sci. NS-47 (3) (2000) 756.
[11] G. Pausch, et al., IEEE Trans. Nucl. Sci. NS-44 (3) (1997) 1040.
[12] L. Bardelli, et al., to be published.
[13] S.W. Smith, The Scientist and Engineer's Guide to Digital Signal Processing, available on www.dspguide.com.
[14] A.V. Oppenheim, R.W. Shafer, Digital Signal Processing, Prentice-Hall, Englewood Cliffs, NJ, 1975.
[15] L. Bardelli, et al., Application of a fast digital sampling system to $\Delta E/E$ identification and subnanosecond timing, Laboratori Nazionali di Legnaro Annual Report, 2002.
[16] G. Pasquali, et al., Nucl. Instr. and Meth. A 301 (1991) 101.